Mechanism of Cohesin Loading onto Chromosomes: A Conformational Dynamics Study

ARTICLE *in* BIOPHYSICAL JOURNAL · AUGUST 2010

Impact Factor: 3.97 · DOI: 10.1016/j.bpj.2010.06.006 · Source: PubMed

2 AUTHORS:

Ozge Kurkcuoglu
Istanbul Technical University
13 PUBLICATIONS **190** CITATIONS
SEE PROFILE

Paul A Bates
The Francis Crick Institute
179 PUBLICATIONS **7,305** CITATIONS
SEE PROFILE

Mechanism of Cohesin Loading onto Chromosomes: A Conformational Dynamics Study

Ozge Kurkcuoglu* and Paul A. Bates*
Biomolecular Modeling Laboratory, Cancer Research UK London Research Institute, Lincoln's Inn Fields Laboratories, London, United Kingdom

ABSTRACT The structure-function relationship of cohesin, an essential chromosome maintenance protein, is investigated by analyzing its collective dynamics and conformational flexibility, enhancing our understanding of the sister chromatid cohesion process. A three-dimensional model of cohesin has been constructed by homology modeling using both crystallographic and electron microscopy image data. The harmonic dynamics of the cohesin structure are calculated with a coarse-grained elastic network model. The model shows that the bending motion of the cohesin ring is able to adopt a head-to-tail conformation, in agreement with experimental data. Low-frequency conformational changes are observed to deform the highly conserved glycine residues at the interface of the cohesin heterodimer. Normal mode analysis further reveals that, near large globular structures such as nucleosome and accessory proteins docked to cohesin, the mobility of the coiled-coil regions is notably affected. Moreover, fully solvated molecular dynamics calculations, performed specifically on the hinge region, indicate that hinge opening starts from one side of the dimerization interface, and is coordinated by highly conserved glycine residues.

INTRODUCTION

During cell division, sister chromatids are held together until the onset of anaphase, a task accomplished by an unusual ringlike protein complex called cohesin. This protein is a member of the structural maintenance of chromosomes (Smc) family, which exists in all eukaryotes (1). Correct sister chromatid cohesion is critical for diverse biological processes such as chromosome condensation (2), gene regulation (3,4), and development (5). Extensive experimental research is devoted to explore the molecular mechanisms underlying the cohesion process; nevertheless, the details of the functional conformational dynamics of cohesin remain unclear.

In yeast, cohesin mainly consists of two Smc proteins, Smc1 and Smc3, each having long anti-parallel coiled-coil regions separating two globular regions, namely an ATP binding head domain and a hinge region (Fig. 1). The two long Smc proteins dimerize from their hinge domains at one end leaving the interacting globular heads at the other end, sandwiching two ATP molecules, to form a functional ABC-type ATPase (6–8). The association and dissociation of the Smc heads are controlled by ATP binding and hydrolysis, respectively (9). Two non-Smc proteins, the kleisin subunit Scc1 and the accessory protein Scc3, are recruited to tether the globular heads of the complex. Cohesin loads onto chromosomes with the help of the evolutionarily conserved loading factor Scc2/Scc4 in yeast, and translocates away toward sites of convergent transcriptional termination (10,11). During cohesion, the cohesin complex topologically entraps the sister chromatids (12,13). At the onset of anaphase, the Scc1 protein is cleaved by separase, a cysteine protease (14,15).

Stable cohesin loading onto chromatin fiber requires the coordinated binding of a number of conserved structural components that are associated with the function of cohesin (16). For example, the ATP activity of cohesin depends on the correct association of the ATPase head, which contains the highly conserved Walker A, Walker B, signature motif and Q loop. These motifs are required for ATP hydrolysis and cohesin binding to chromatin, as shown by mutation studies on the ATP binding site (17). Another essential component is the kleisin subunit Scc1, which not only connects the two Smc heads but also stimulates ATP hydrolysis (18). Moreover, in the hinge region, several highly conserved glycine residues at the Smc proteins' dimerization interface have been shown to be critical for efficient binding to DNA (19,20).

Although the overall structural mechanism of chromatin entrapment by cohesin is still under debate, one essential feature is clear: the cohesin heterodimer ring complex is expected to contain an entry gate, which opens to entrap the chromatin. Along with other observations on *Escherichia coli* condensin MukB (21,22), a recent structural study suggested that ATP-mediated head-domain association triggers the detachment of the C-terminal of MukF (non-Smc subunit) bound to the MukB head, creating an entry gate into the ring (23). Similarly for yeast, an early model for loading was proposed based on the entry gate being located between the Smc1 and Smc3 head regions (24). This possibility has been tested by artificially cross-linking Scc1 to the head domain (25). However, the analysis showed that the detachment of the head domains was not necessary for cohesin loading, but instead, the hinge subunit interface opens to allow the passage of the chromatin fiber (Fig. 1 *C*), which

Submitted February 25, 2010, and accepted for publication June 3, 2010.

*Correspondence: ozge.kurkcuoglu@cancer.org.uk or paul.bates@cancer.org.uk

Editor: Ruth Nussinov.

0006-3495/10/08/1212/9 $2.00

doi: 10.1016/j.bpj.2010.06.006

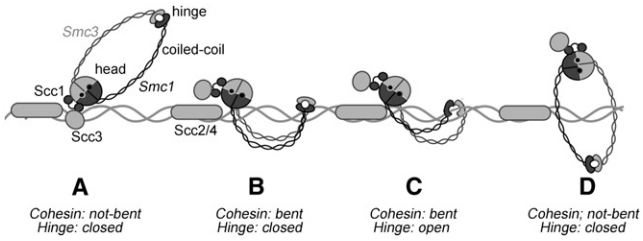

FIGURE 1 Schematic representation of cohesin and, the most likely model for its loading mechanism to chromatin (25). Cohesin is formed of Smc1 and Smc3 proteins dimerized from a hinge region from one end leaving two globular heads at the other end forming a functional ABC-type ATPase. The kleisin subunit Scc1 and the accessory protein Scc3 bind cohesin from the head region. (*A* and *B*) Cohesin loads onto chromatin fiber with the assistance of a loading factor Scc2/Scc4 in yeast. (*C*) The hinge opens to entrap the fiber inside the ring. (*D*) Cohesin translocates away from the loading factor. Illustrated conformations of the cohesin ring and the hinge region are generated and analyzed in this study.

indicates that the loading mechanism of cohesin for prokaryotes is likely to differ from that of eukaryotes. Available open crystal structures of the eukaryotic hinge also suggests that the hinge region may undergo a transient stepwise opening, first from one side of the interface, and then from the other (7,26). However, the latter structural study (26) indicates that the open hinge structure also may be due to the instability of one of the dimerization sites because of the missing coiled-coil domains in the construct. On the other hand, there is some evidence to suggest the hinge opening is facilitated by the communication between the hinge and head regions, as experiments in bacteria showed that an initial interaction of the hinge domain with DNA, triggered ATP hydrolysis at the ATPase head (20). All the above observations imply that cohesin undergoes significant conformational changes to create an entry gate upon loading onto chromatin.

In fact, various electron microscopy (EM) (6) and atomic force microscopy images (27,28) reveal the dramatic conformational changes the Smc proteins can undergo. Cohesin displays a variety of coiled-coil arm conformations (6). Moreover, there is evidence for direct interaction between Smc head and hinge regions (27–29). Interestingly, for various functional purposes, similarly-structured molecules containing long coiled-coil domains adopt head-to-tail conformations, such as the human Rad50/Mre11/Nbs1 complex (30), and the kinesin-1 motor protein (31).

To our knowledge, a detailed computational study on the complete structure of cohesin has not previously been attempted. Nevertheless, analogous functional parts to cohesin have been studied from a computational perspective. The ATPase head of the Smc proteins are structurally similar to ABC transporters and share the same motifs at the ATP binding site. The structural and functional dynamics of the ABC-type proteins have been extensively investigated with computational techniques such as molecular dynamics (MD) (32,33) and normal mode analysis (33,34). These studies give insights into the ATP activity of cohesin. According to EM images, the coiled-coil arms of cohesin are spread, resulting in a unique ringlike shape (6). The low-frequency dynamics of a similarly shaped molecule, a circular DNA molecule, have been studied with normal mode analysis (35), pointing out the elastic rod properties of the macromolecule with intrinsic bending, twisting, and stretching motions. Similarly, long F-actin filaments with almost the same length of long coiled-coil arms displayed by cohesin exhibit the same elastic rod properties observed by normal mode analysis (36).

Coarse-grained elastic network models, using normal mode analysis, are simple yet powerful computational tools to explore the collective dynamics of large biological macromolecules around their native conformations (37–40). For these coarse-grained models, the macromolecular structure is described as an elastic network in which each node may be represented by a single point, usually being the C_α atom of residues (41–43), or by a group of residues (44–46). Here, each neighboring node is connected by a harmonic spring, and the mechanical motions of the protein complexes are calculated using a uniform harmonic potential. These coarse-grained elastic network models can successfully predict the functional dynamics of very large macromolecules such as the GroEL-GroES complex (47–49), the RNA polymerase (50), the ribosome complex (51–53), and the satellite tobacco mosaic viral capsid (54), where a full-atom technique such as MD is computationally unaffordable. These studies show that high-resolution structures of macromolecules are not necessary to predict their low-energy motions, which are often related to their biological functions (55,56).

In this study, our aim is to reveal the missing molecular details of how the two halves of the hinge may open to create an entry gate on yeast cohesin for DNA. Here, we focus on:

1. The collective motions of the whole ring structure that may contribute to opening of the large ring, investigated with the coarse-grained elastic network model.
2. The effect of binding of large densities (e.g., a nucleosome particle) on the collective dynamics of cohesin.
3. Higher molecular details of the hinge region dynamics leading to an open hinge conformation, monitored with fully solvated MD simulations.

Finally, based on our results, we propose a likely mechanism for the loading of cohesin to chromatin fiber.

METHODS

There are no complete three-dimensional structures of Smc proteins. However, this protein family is evolutionarily conserved, and it is possible to find structural information on the ATPase head and hinge region of the macromolecule from various species (7,8,23,57). Based on the available structural data, the three-dimensional structure of the head and hinge

domains were modeled for yeast cohesin by the automated protein structure prediction web-server 3D-JIGSAW (58) (see Fig. S1 *A* in the Supporting Material). On the other hand, existing modeling techniques are incapable of accurately constructing the long coiled-coil arms based on amino-acid sequence. Therefore, the cohesin ring was completed by simply inserting the anti-parallel coiled-coil fragment of the tropomyosin molecule from pig cardiac muscle (PDB code (59): 1c1g (60)), between the short coiled-coils emerging from the head and the hinge domains. There are conserved short breaks along the coiled-coils from which flexible loops protrude (61). However, these loops do not affect the conformational deformations of cohesin calculated by the elastic network model at the lowest-frequencies (Fig. S2); as a result, they are not included in the model. The details of modeling yeast cohesin structure can be found in the Supporting Material.

To observe the effect of specific regions on the dynamics of the complex using the coarse-grained elastic network model, various cohesin model systems were generated from the above-constructed cohesin model. The model systems are:

1. The cohesin complex with ATP.Mg^{2+}, which is called SMC1-3.
2. The cohesin complex with a nucleosome bound to the head domain with ATP.Mg^{2+}, which is called SMC1-3_nuc_to_head.
3. The cohesin complex with a nucleosome bound to the coiled-coil regions with ATP.Mg^{2+}, which is called SMC1-3_nuc_to_coil (Fig. S1 *B*).

The low-frequency conformational dynamics of cohesin were investigated using the anisotropic network model (ANM) (42). The elastic network for the cohesin structure was constructed placing single point masses, i.e., nodes, located at the C_α position of amino acids and *P* position of nucleotides. All neighboring nodes were linked pairwise by a harmonic spring γ_{ij}, the value of which is assigned based on total number of atom-atom interactions between node i and j within a cutoff distance r_{cut} of 10 Å, assuming that the harmonic forces are acting in parallel to one another (62). The potential energy of the network of N nodes was then given by the summation over the harmonic interactions of (i,j) pairs,

$$V = (1/2)\sum_{i,j}^{r_{cut}} \gamma_{ij}\left(R_{ij} - R_{ij}^{0}\right)^2, \qquad (1)$$

where R_{ij} and $R_{ij}{}^0$ are the instantaneous and equilibrium distances between nodes i and j ($1 \leq i,j \leq N$). The diagonalization of the mass-weighted Hessian matrix, including the connectivity information of the (i,j) pairs, leads to the calculation of $3N$-6 vibrational motions of the protein structure, where rotational and translational motions were neglected (see the Supporting Material for details).

New conformation of cohesin ring was generated by deforming the native structure along the positive direction of the lowest frequency motion calculated with ANM. The generated coarse-grained structure of cohesin was then completed by rigidly displacing heavy atoms in the direction of their C_α atom displacement vectors. Then the structure was relaxed by energy minimization using AMBER 9 (63) using the ff03 force-field parameters (64). This so-called reverse-mapping technique is explained in detail elsewhere (65).

For higher levels of detail, fully solvated MD simulations, using the MD package NAMD 2.6 (66) with the CHARMm22 force field (67,68), were performed on various hinge structures and for a simulation time of 20 ns (see Supporting Material).

RESULTS AND DISCUSSION

To our knowledge, the molecular details of the loading process are not well known; however, for this event to be realized, a large conformational change of the yeast cohesin ring, i.e., opening of the hinge dimerization interface, would be required. Therefore, this study is mainly focused on revealing the detailed structural dynamics of the cohesin ring and the specific conformational changes of the hinge region, during the loading process. To validate the general approach, and to gain a deeper understanding of the coupling between motion and function of yeast cohesin, the complete cohesin model was investigated by a coarse-grained elastic network model (see Methods). Then, various hinge conformations were generated from normal mode analysis and in silico point mutations, and the opening of the DNA entry gate monitored by MD simulations. The results of this analysis are given and discussed in the following sections.

Cohesin dynamics

Elastic rod properties of the cohesin ring

The low-frequency dynamics of the complete modeled ringlike cohesin structure were explored by the elastic network model using normal mode analysis. The flexibility of the 50-nm-long coiled-coil arms connecting the head and hinge regions dominate the collective motions of the cohesin molecule in the lowest part of the frequency spectrum. For the complete ringlike structure, the first 10 and 100 normal modes contribute 95% and 99% of the total conformational change, respectively. The mean-square fluctuations (msf) averaged over the first 10 and 100 normal modes are shown for the cohesin model SMC1-3 (Fig. 2 *A*). The coiled-coil arms exhibit high mobility compared to the ATPase head and the hinge, whereas the smaller hinge region is more mobile compared to the head region. Moreover, conserved breaks in yeast, namely, loop3 (Cys^{944}-Lys^{990}) on Smc1 and loop 2 (Lys^{387}-Ile^{403}) and loop3 (Gly^{958}-Ser^{970}) on Smc3 along the coiled-coils, appear to increase the flexibility of the 50-nm-long arms that can lead to specific kinks as previously observed for Smc proteins (6) (Fig. S2). However, these breaks do not alter the directions of the normal modes in the low-frequency range; the overlap value (69) averaged over the first 10 normal modes is 0.99.

The lowest-frequency motions of the ringlike cohesin correspond to different combinations of bending, stretching, and twisting motion of the cohesin (Fig. 2 *B*), similar to the low-frequency motions of a circular DNA (35). The collectivity coefficients (70) of the first three nonzero slow modes are, respectively, 0.75 (bending), 0.51 (stretching), and 0.75 (twisting), indicating that a high fraction of residues contributes to these conformational changes. When the collectivity of a single mode is high, usually this mode alone can describe the large conformational transition of the protein from an open to a closed conformation on its way to fulfill its biological function (70). For the case of the cohesin molecule, considering the high amplitude motions and highly collective nature of the first three normal modes, the ringlike molecule is most likely to undergo a set of functionally important bending-stretching-twisting motions when it is free in solution. These motions are extended when the ringlike molecule is constrained from one part of its body, as will be discussed in the following section.

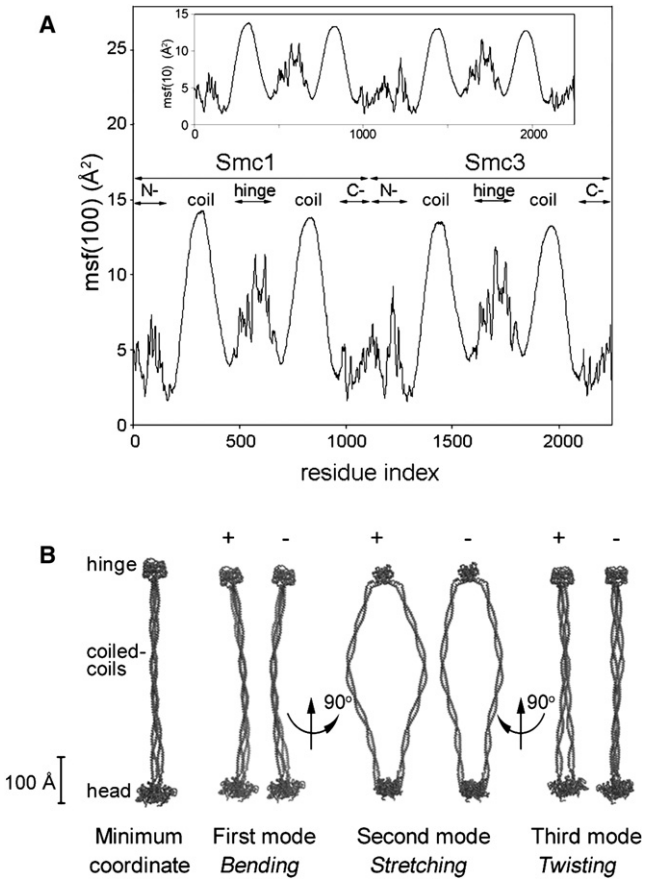

FIGURE 2 (*A*) The mean-square fluctuations (msf) averaged over the first 100 normal modes (msf(100)) for the cohesin model SMC1-3 is given with functional sites indicated. (*Inset plot*) Msf averaged over the first 10 normal modes (msf(10)) for the same model, which contribute 95% of the overall motion. (*B*) The minimum coordinates and the alternative directions (±) of the first three normal mode deformations of the cohesin model are shown in ribbon presentations. A scale bar is given to indicate the relative scale of the cohesin model. All molecular graphics are generated with PyMol molecular viewer (DeLano Scientific, Palo Alto, CA; http://www.pymol.org/).

The orientational cross-correlation map averaged over the first 10 and 100 normal modes for the cohesin dimer is shown in Fig. S3. Collective motions of the head and the hinge regions are not correlated (correlation coefficient ~0.2). This is perhaps expected, as these regions are separated by 50-nm arms; and as shown above, they are quite flexible and undergo various motions determining the conformational flexibility of the cohesin molecule. Indeed, this observation suggests that it is unlikely that any activity on the head region, such as ATP hydrolysis, would be effectively transmitted to the hinge over such a distance, unless they are in very close proximity.

Effect of a large globular subunit on cohesin dynamics

EM images reveal that the kleisin subunit Scc1 and the accessory protein Scc3 bind cohesin from the head region (6). Moreover, it is known that a loading factor called Scc2/Scc4 in yeast assists cohesin to load onto chromatin fiber (10,11,16,17) (see Fig. 1). A large mass docked to one part of the molecule would change the overall flexibility of the dimer. For elastic network models, where the whole structure is considered as a uniform material, low energy normal mode deformations of macromolecules are determined by their size and shape, not by specific atomic properties. Even with the simplification of structures, such models are very successful in predicting functional motions of macromolecules (38,39). Therefore, the effect of a large density on the fluctuations of cohesin can be investigated by an elastic network model, purely from a structural mechanics perspective, and the low energies can be investigated to illuminate functional motions.

Crystal structures of the kleisin subunit Scc1, the accessory protein Scc3, and the loading factor Scc2/Scc4 are not available. However, a nucleosome particle should be proximal to the loading factor, and consequently to the cohesin complex, upon cohesin loading; therefore, a nucleosome molecule (PDB code: 1p3i (71)) is manually placed next to the head region, solely to represent a large globular density docked to the head domain (SMC1-3_nuc_to_head, Fig. S1 *B*). Specific interactions between the nucleosome and the cohesin are not considered, but steric clashes are prevented. The msfs averaged over the first 100 modes are compared for the models SMC1-3 and SMC1-3_nuc_to_head in Fig. S4 *B*. The presence of a large density next to the head region, in various positions and orientations (Fig. S4), increases the flexibility of the coiled-coil arms, as well as the mobility of the hinge region. In the hinge region, the major deformation is concentrated on the highly conserved glycine residues at the dimerization interface. This is more pronounced than for the model SMC1-3, thereby indicating hinge opening is facilitated in the former case. As expected, as they are neighboring the nucleosome, the regions close to the nucleosome particle on the periphery of the head domain fluctuate less compared to the SMC1-3 model. Global motions such as bending, stretching, and twisting of the cohesin SMC1-3 model are preserved in the SMC1-3_nuc_to_head model, with an overlap value (69) of 0.93 (averaged over the first 10 normal modes).

The collective motions of cohesin once loaded onto the chromatin fiber are also investigated with the elastic network model. For this purpose, one nucleosome particle is manually placed between the coiled-coil arms of cohesin near the head region, preventing steric clashes (SMC1-3_nuc_to_coil, Fig. S1 *B*). Due to the presence of a large density between the arms of cohesin, the head and the hinge region fluctuations slightly increase compared to the SMC1-3 model, while the coiled-coil regions close to the nucleosome particle are significantly stabilized (Fig. S5 *B*). This effect along the coiled-coil regions is also observed for the cohesin models with a nucleosome particle placed at different positions between the arms (Fig. S5). The system undergoes similar conformational changes to the SMC1-3 model, indicated

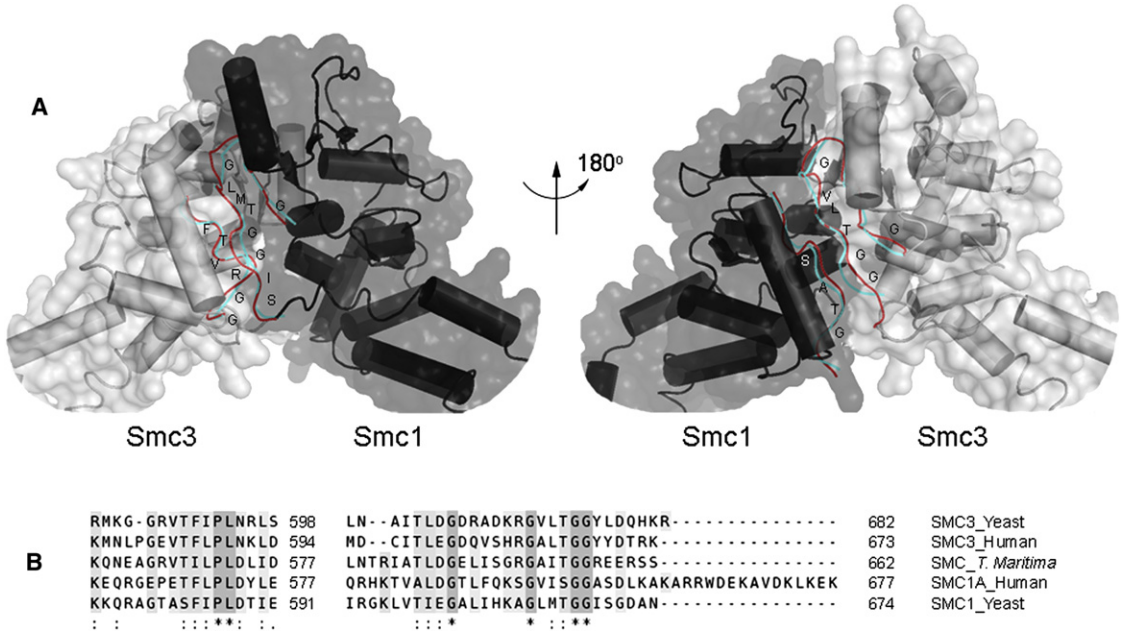

FIGURE 3 Lowest frequency motion of cohesin corresponds to the bending motion from the middle of the coiled-coil arms, eventually adopting a head-to-tail conformation. Alternative directions (±) (*cyan* and *red* colors at the dimerization interface, respectively) of the slowest mode are shown for the cohesin molecule at the hinge region. (*A*) The backbone at the dimerization interface deforms at the highly conserved glycine residues. (*B*) The evolutionarily conserved glycine residues are shown where sequences are aligned for yeast, human, and *Thermotoga maritima*.

by a high overlap of 0.87 (calculated over the first 10 normal modes).

Bending motion of cohesin is needed to obtain head-to-tail conformation

The most significant conformational change observed for cohesin is a transition from a ring conformation to a head-to-tail conformation due to the bending motion of the coiled-coil arms (27,28). This finding is also supported by Förster resonance energy transfer studies (29). Accordingly, the first normal mode of cohesin dynamic corresponds to the bending motion of the molecule from its middle, near the conserved breaks on the coiled-coils, namely loop 2 on Smc3 and loops 3 on both proteins (Fig. 1 *B*, Fig. 2 *B*, and Fig. S2 *B*). Interestingly, this bending motion is commonly used for various functional purposes in other molecules that have a similar architecture (30,31).

In Fig. 3 *A*, two alternative conformations for the bending motion are superimposed based on the backbone of the hinge region. Interestingly, the dimerization interface within the hinge domain is slightly deformed around the evolutionarily conserved glycine residues and on both sides of the interface, namely Gly^{663}, Gly^{667}, and Gly^{668} on Smc1 and Gly^{670}, Gly^{674}, and Gly^{675} on Smc3 (Fig. 3, *A* and *B*). The transition region between the hinge and the coiled-coils exhibits high structural deformation (not shown). This appears to disrupt the stability of the β-sheets, which cross the interface at both sides of the hinge, especially $\beta 3$, $\beta 7$, and $\beta 8$ on both Smc proteins (see Fig. S1), thereby causing the cohesin dimer to open. This structural deformation is also observed in the second (stretching) and third (twisting) modes (not shown). Moreover, as discussed above, hinge region fluctuations and consequently, hinge interface deformation, increase when the cohesin ring is docked to a large mass at its head region. The conserved glycine residues are highly critical for the dimerization of the Smc molecules as well as for a more stable coiled-coil arm conformation (20). Accordingly, our results suggest that these residues appear to be important for maintaining the flexibility of the dimerization interface when it is free in solution, and to coordinate the dissociation of the hinge when it binds to chromosome.

Molecular dynamics simulations of the cohesin hinge

Mutation of the conserved glycine residues causes the hinge to open

To monitor residue fluctuations at the hinge interface, the hinge domain of wild-type yeast cohesin is simulated by MD for a time course of 20 ns. Although outer loops and short coiled-coil regions display high amplitude motions, the hinge interface is very flexible due to the highly conserved glycine residues listed above and shown in Fig. 3 *B*; these absorb high-amplitude fluctuations to maintain the stability of the dimer interface (Movie S1). An earlier study (19) reported that simultaneous mutation of these conserved glycine residues to aspartic acid prevents the dimerization of bacterial cohesin. Similarly for the yeast cohesin hinge domain, mutating, in silico, glycine residues

to aspartic acids at both sides of dimerization disturbs the hinge structure. The hinge opens from the stable β-sheets, between β7 and β8 on both Smc proteins, at a very early stage of the simulation at ~1 ns, adopting an open conformation from one side of the interface and a less open conformation from other side (Fig. 4 *A* and Movie S2). As shown in Fig. 4 *C*, the distance between two residues at the base of the β-sheets, i.e., Ala^{657} (β7) and Gly^{667} (β8) on Smc1, and Asp^{664} (β7) and Gly_{674} (β8) on Smc3, increases from 4.7 Å to 8.2 Å at one side of the hinge (side 1, on Smc1) and to 16.6 Å at the other (side 2, on Smc3) at ~3 ns. This conformation of the yeast cohesin hinge is very similar to the open structure of bacterial hinge (7), with similar distances to those monitored above, 4.4 Å (closed conformation, PDB code: 1gxl) and 16.2 Å (open conformation, PDB code: 1gxj) at one side of dimerization. This finding strongly suggests that at least for eukaryotes, the cohesin-hinge opening mechanisms are likely to be conserved and coordinated by these highly conserved glycines.

To reveal the importance of the location of each conserved glycine residue at dimerization interface (Fig. 3 *B*), note that they are mutated, in silico, one pair at a time. Mutating the paired residues Gly^{667} on Smc1 and Gly^{674} on Smc3, or Gly^{668} on Smc1 and Gly^{675} on Smc3 to aspartic acid, results in the structural deformation of the interdomain bridging β-sheets due to interruption in the H-bonding network here (see Movie S3 and Movie S4). More-detailed analysis suggests that Gly^{667} on Smc1 and Gly^{674} on Smc3 are mainly responsible for the β-sheet interface opening from both dimerization sides. On the other hand, mutating the paired residues Gly^{663} on Smc1 and Gly^{670} on Smc3 alone do not cause any significant deformations of the hinge (not shown).

Simulations of a bent conformation for cohesin indicate hinge opening

Based on our normal mode analysis of cohesin, during bending motion of the ring-shaped molecule, the hinge region does not undergo a major domain motion, such as from a closed to an open hinge conformation; but rather, some residue-residue interactions are weakened or lost, especially on outer loops and most importantly, at the β-sheets linking both sides of the dimerization interface (not shown). To investigate whether these contact losses within the hinge region may cause the cohesin ring to fully open, a new conformation of the hinge is generated from one alternative direction of the slowest mode deformation (see Fig. 2 *B*).

The wild-type hinge structure from a significantly bent conformation of cohesin (~45° from a planar ring schematically shown in Fig. 1 *B*), generated by four subsequent steps of ANM and energy minimization (see Supporting Material), is simulated by MD for a time course of 20 ns. The root mean-square deviation between the hinge from the planar ring structure and the above bent conformation was 2.7 Å (based on backbone root mean-square deviation). The number of H-bonds stabilizing the β-sheets at the dimerization interface is smaller during the MD simulation of the hinge from the bent conformation when compared to the hinge from the not-bent conformation. This disruption in the H-bonding network within β-sheets β7 and β8 causes the hinge to open from both sides, and furthermore to extend the opening only from one side at ~1 ns, to reveal a highly

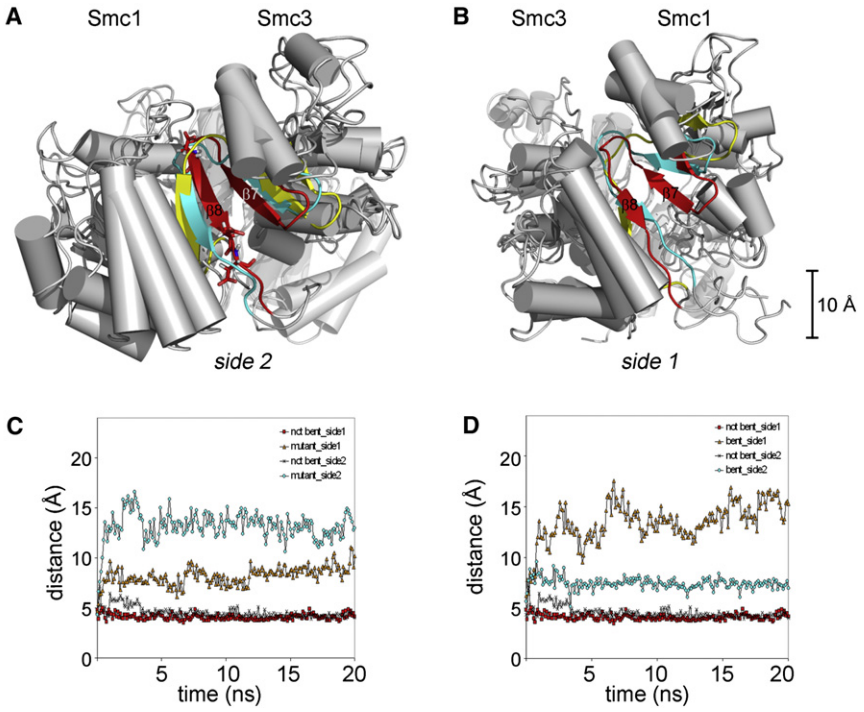

FIGURE 4 Molecular dynamics trajectory analysis for (*A*) mutated hinge structure and (*B*) a hinge structure from bent cohesin conformation. Mutations of three highly conserved glycine residues are shown with sticks. Several conformations are superimposed to observe the opening of the β-sheets bridging the interface for (*A*) mutated hinge structure at 0 ns (*red*), 0.4 ns (*cyan*), and 7 ns (*yellow*); and (*B*) hinge structure from bent cohesin conformation at 0 ns (*red*), 0.7 ns (*cyan*), and 7 ns (*yellow*). Distances monitored across the intramolecular β-sheets, located on either side of the interface, i.e., between C_α atoms of Ala^{657} and Gly^{667} on Smc1, and Asp^{664} and Gly^{674} on Smc3, are plotted for (*C*) mutated hinge structure and (*D*) hinge structure from bent cohesin conformation, compared with results for hinge structure from not-bent cohesin.

positive surface inside the hinge, a region that may subsequently interact with DNA (Fig. 1 *C*, Fig. 4, *B* and *D*, Fig. S6, and Movie S5).

MD simulations on both mutated hinge structures and the bent-ring conformations suggest that the yeast cohesin hinge opens more from one side of the dimerization interface than the other. This is clearly observed from the first principal component calculated over the first 5 ns of the MD trajectory, during which the most significant structural changes of the hinge are observed (Fig. S7). A rotational motion on one-half of the hinge is observed to open the weakened β-sheet between β7 and β8, either by mutations or caused by the bending motion of cohesin. The other part of the β-sheet (β4-β6), being freer to move, easily translocates away to cause an open hinge conformation. However, this does not exclude the possibility of opening of the other side at a latest stage, due to high amplitude motions of the coiled-coils or interaction with DNA. Indeed, opening of the one side or the other is likely to be equally possible, particularly due to the harmonic motion of cohesin ring (in a positive or negative direction of bending). These results agree with the PiSQRD server (72) and TLSMD server (73), both of which were used to analyze the protein's flexibility and quasirigid dynamic domains. Essentially, residues Gly^{656}-Ile^{659} (β7) and Gly^{663}-Gly^{667} (β8) on Smc1 (Gly^{663}-Ala^{666} and Gly^{670}-Gly^{674} on Smc3) belong to different dynamic domains and move in opposite directions, which eventually disturb the H-bonding network, and lead to an open conformation of the hinge as discussed.

Proposed model for the mechanism of cohesin loading onto chromatin

Cohesin loading onto chromatin fiber appears to be coordinated by the collective motions of the complex, but primarily by the lowest-frequency bending motion of the coiled-coils. Considering the results from our normal mode and MD analysis discussed above, the mechanism of yeast cohesin loading onto chromatin fiber appears to agree with the transient hinge opening model (25). Cohesin initially interacts on or near the loading protein complex Scc2/Scc4 on the chromatin fiber, probably near the head region (16). Constraining the head region results in increasing mobility of the hinge and coiled-coil arms, enabling cohesin to change its conformation and to bend toward the chromatin fiber, facilitated by the conserved breaks along the arms. This motion of the cohesin molecule deforms the flexible dimerization interface at the hinge region, resulting in a transient opening of the dimer, revealing a highly positive patch inside the hinge; complete opening of the hinge may be further facilitated by the interaction of this patch with DNA. Once the chromatin fiber enters the ring, it stabilizes the fluctuations of the coiled-coil arms from where it interacts. The intrinsic mobility of the hinge region helps the ring to reclose entrapping the chromatin fiber inside. Ultimately, on the onset of mitosis a second chromatin fiber will reside within the ring; two sister chromatids are encircled. As to whether the second chromatin fiber is replicated from the first or the ring opens a second time to capture a sister chromatid, has not been experimentally elucidated. The latter phase is not the purpose of this study, which focuses solely on initial cohesin loading onto a single fiber. Nevertheless, as can be seen from Fig. S1 *B*, there is ample space to fit a second fiber within the cohesin ring structure.

CONCLUSIONS

Protein structures have evolved in such a way that they ensure the robustness of biological processes to sustain cellular life. For the evolutionarily conserved cohesin, its highly collective functional motions, such as bending, stretching, and twisting, are intrinsic properties of the cohesin structure, which provides the necessary tools (i.e., an ATPase head, long arms, and a hinge) to carry out ATP hydrolysis, topologically entrap sister chromatids, and create an entry gate for the chromatin fiber when necessary.

The elastic network model suggests that the stiffness of the coiled-coils is modulated by their environment such as binding of a large density, such as Scc1, Scc3, and Scc2/Scc4, or a nucleosome particle. Significant conformational changes in the coiled-coils will bring the hinge domain into close proximity with the head domain, an essential requirement if ATP hydrolysis were needed to trigger complete hinge opening; as shown by our orientational cross-correlation maps, there is a lack of effective indirect communication between the head and hinge region via the flexible 50-nm coiled-coils. An alternative reason for the ATPase activity may be to detach the ATPase head from its loading factor, similar to a kinesin molecule with a coiled-coil and head structure that, before its next step, detaches itself from microtubule after ATP hydrolysis (74).

The yeast cohesin hinge seems to be in a pseudo-stable state, where its small hinge dimerization interface is very sensitive to structural changes within the region of the highly conserved glycine residues (Gly^{663}, Gly^{667}, and Gly^{668} on Smc1; and Gly^{670}, Gly^{674}, and Gly^{675} on Smc3). These glycines are located at strategic positions within the interface and appear to absorb any excessive energy originating from the motions of the coiled-coils and outer loops, thereby keeping the interface closed. The pseudo-stable state of the hinge may be energetically shifted to the stable or the unstable side of the equilibrium, by making mutations to the conserved residues within the hinge region, and/or by bending the cohesin ring, respectively. Effective dimerization of Smc proteins, to form this unusually small nonobligate heterodimer interface (75), is likely to be dependent on these glycine residues along with a conserved pattern of hydrophobic residues. Similar to other heterodimer interactions (76), the hydrophobic

residues (Ala^{582}, Phe^{584}, Ile^{585}, Leu^{664}, and Met^{665} on Smc1; and Val^{589}, Phe^{591}, Ile^{592}, Val^{671}, and Leu^{672} on Smc3) are clustered at the central interface, with the highly conserved glycines located on both sides and at the periphery of the interface (Fig. 3 *B*). This pattern implies that the first contacts between Smc1 and Smc3 hinge regions are due to π-interactions between the hydrophobic residues. Then, the flexible glycines seem to have a structural role to finalize the H-bonding network across the β-sheets bridging the interface and thereby maintain the stability of cohesin.

Understanding cohesin dynamics is essential in deciphering the sister chromatid cohesion process, and to understand the molecular mechanism underlying severe developmental disorders such as Cornelia de Lange syndrome. The structures and functional sites of Smc proteins are evolutionarily conserved; therefore, our findings on cohesin dynamics may contribute to understanding other Smc proteins, in particular condensin, which has an important role in chromosome condensation.

SUPPORTING MATERIAL

Five equations, one table, seven figures, and five movies are available at http://www.biophysj.org/biophysj/supplemental/S0006-3495(10)00715-0.

The authors thank Frank Uhlmann for many stimulating discussions on cohesin and its functions, and Pemra Doruker for detailed discussions on the elastic network model used in this study. The elastic networks program code was developed at Polymer Research Center in Bogazici University. The authors also thank members of the Biomolecular Modeling Laboratory for useful discussions.

This work was funded by Cancer Research UK.

REFERENCES

1. Nasmyth, K., and C. H. Haering. 2009. Cohesin: its roles and mechanisms. *Annu. Rev. Genet.* 43:525–558.
2. Guacci, V., D. Koshland, and A. Strunnikov. 1997. A direct link between sister chromatid cohesion and chromosome condensation revealed through the analysis of MCD1 in *S. cerevisiae*. *Cell.* 91:47–57.
3. Pauli, A., F. Althoff, …, K. Nasmyth. 2008. Cell-type-specific TEV protease cleavage reveals cohesin functions in *Drosophila* neurons. *Dev. Cell.* 14:239–251.
4. Schuldiner, O., D. Berdnik, …, L. Luo. 2008. piggyBac-based mosaic screen identifies a postmitotic function for cohesin in regulating developmental axon pruning. *Dev. Cell.* 14:227–238.
5. Revenkova, E., M. L. Focarelli, …, A. Musio. 2009. Cornelia de Lange syndrome mutations in SMC1A or SMC3 affect binding to DNA. *Hum. Mol. Genet.* 18:418–427.
6. Anderson, D. E., A. Losada, …, T. Hirano. 2002. Condensin and cohesin display different arm conformations with characteristic hinge angles. *J. Cell Biol.* 156:419–424.
7. Haering, C. H., J. Löwe, …, K. Nasmyth. 2002. Molecular architecture of SMC proteins and the yeast cohesin complex. *Mol. Cell.* 9:773–788.
8. Haering, C. H., D. Schoffnegger, …, J. Löwe. 2004. Structure and stability of cohesin's Smc1-kleisin interaction. *Mol. Cell.* 15:951–964.
9. Hirano, M., and T. Hirano. 2004. Positive and negative regulation of SMC-DNA interactions by ATP and accessory proteins. *EMBO J.* 23:2664–2673.
10. Ciosk, R., M. Shirayama, …, K. Nasmyth. 2000. Cohesin's binding to chromosomes depends on a separate complex consisting of Scc2 and Scc4 proteins. *Mol. Cell.* 5:243–254.
11. Lengronne, A., Y. Katou, …, F. Uhlmann. 2004. Cohesin relocation from sites of chromosomal loading to places of convergent transcription. *Nature.* 430:573–578.
12. Ivanov, D., and K. Nasmyth. 2005. A topological interaction between cohesin rings and a circular minichromosome. *Cell.* 122:849–860.
13. Haering, C. H., A. M. Farcas, …, K. Nasmyth. 2008. The cohesin ring concatenates sister DNA molecules. *Nature.* 454:297–301.
14. Uhlmann, F., F. Lottspeich, and K. Nasmyth. 1999. Sister-chromatid separation at anaphase onset is promoted by cleavage of the cohesin subunit Scc1. *Nature.* 400:37–42.
15. Uhlmann, F. 2003. Chromosome cohesion and separation: from men and molecules. *Curr. Biol.* 13:R104–R114.
16. Tóth, A. H., R. Ciosk, …, K. Nasmyth. 1999. Yeast cohesin complex requires a conserved protein, Eco1p(Ctf7), to establish cohesion between sister chromatids during DNA replication. *Genes Dev.* 13: 320–333.
17. Arumugam, P., S. Gruber, …, K. Nasmyth. 2003. ATP hydrolysis is required for cohesin's association with chromosomes. *Curr. Biol.* 13:1941–1953.
18. Arumugam, P., T. Nishino, …, K. Nasmyth. 2006. Cohesin's ATPase activity is stimulated by the C-terminal Winged-Helix domain of its kleisin subunit. *Curr. Biol.* 16:1998–2008.
19. Hirano, M., and T. Hirano. 2002. Hinge-mediated dimerization of SMC protein is essential for its dynamic interaction with DNA. *EMBO J.* 21:5733–5744.
20. Hirano, M., and T. Hirano. 2006. Opening closed arms: long-distance activation of SMC ATPase by hinge-DNA interactions. *Mol. Cell.* 21:175–186.
21. Ku, B., J.-H. Lim, …, B. H. Oh. 2010. Crystal structure of the MukB hinge domain with coiled-coil stretches and its functional implications. *Proteins.* 78:1483–1490.
22. Li, Y., A. J. Schoeffler, …, M. G. Oakley. 2010. The crystal structure of the hinge domain of the *Escherichia coli* structural maintenance of chromosomes protein MukB. *J. Mol. Biol.* 395:11–19.
23. Woo, J. S., J. H. Lim, …, B. H. Oh. 2009. Structural studies of a bacterial condensin complex reveal ATP-dependent disruption of intersubunit interactions. *Cell.* 136:85–96.
24. Gruber, S., C. H. Haering, and K. Nasmyth. 2003. Chromosomal cohesin forms a ring. *Cell.* 112:765–777.
25. Gruber, S., P. Arumugam, …, K. Nasmyth. 2006. Evidence that loading of cohesin onto chromosomes involves opening of its SMC hinge. *Cell.* 127:523–537.
26. Griese, J. J., G. Witte, and K.-P. Hopfner. 2010. Structure and DNA binding activity of the mouse condensin hinge domain highlight common and diverse features of SMC proteins. *Nucleic Acids Res.* 38:3454–3465. 10.1093/nar/gkq038.
27. Yoshimura, S. H., K. Hizume, …, M. Yanagida. 2002. Condensin architecture and interaction with DNA: regulatory non-SMC subunits bind to the head of SMC heterodimer. *Curr. Biol.* 12:508–513.
28. Sakai, A., K. Hizume, …, M. Yanagida. 2003. Condensin but not cohesin SMC heterodimer induces DNA reannealing through protein-protein assembly. *EMBO J.* 22:2764–2775.
29. Mc Intyre, J., E. G. D. Muller, …, F. Uhlmann. 2007. In vivo analysis of cohesin architecture using FRET in the budding yeast *Saccharomyces cerevisiae*. *EMBO J.* 26:3783–3793.
30. Moreno-Herrero, F., M. de Jager, …, C. Dekker. 2005. Mesoscale conformational changes in the DNA-repair complex Rad50/Mre11/Nbs1 upon binding DNA. *Nature.* 437:440–443.
31. Dietrich, K. A., C. V. Sindelar, …, S. E. Rice. 2008. The kinesin-1 motor protein is regulated by a direct interaction of its head and tail. *Proc. Natl. Acad. Sci. USA.* 105:8938–8943.

32. Campbell, J. D., S. S. Deol, …, M. S. Sansom. 2004. Nucleotide-dependent conformational changes in HisP: molecular dynamics simulations of an ABC transporter nucleotide-binding domain. *Biophys. J.* 87:3703–3715.

33. Jones, P. M., and A. M. George. 2007. Nucleotide-dependent allostery within the ABC transporter ATP-binding cassette: a computational study of the MJ0796 dimer. *J. Biol. Chem.* 282:22793–22803.

34. Weng, J., J. Ma, …, W. Wang. 2008. The conformational coupling and translocation mechanism of vitamin B12 ATP-binding cassette transporter BtuCD. *Biophys. J.* 94:612–621.

35. Matsumoto, A., I. Tobias, and W. K. Olson. 2005. Normal mode analysis of circular DNA at the base-pair level. 1. Comparison of computed motions with the predicted behavior of an ideal elastic rod. *J. Chem. Theory Comput.* 1:117–129.

36. Ma, J. P. 2006. Applications of normal mode analysis in structural refinement of supramolecular complexes. *In* Normal Mode Analysis, Theory and Applications to Biological and Chemical Systems. Q. Cui and I. Bahar, editors. Chapman & Hall/CRC, New York.

37. Tirion, M. M. 1996. Large amplitude elastic motions in proteins from a single-parameter, atomic analysis. *Phys. Rev. Lett.* 77:1905–1908.

38. Bahar, I., and A. J. Rader. 2005. Coarse-grained normal mode analysis in structural biology. *Curr. Opin. Struct. Biol.* 15:586–592.

39. Ma, J. P. 2005. Usefulness and limitations of normal mode analysis in modeling dynamics of biomolecular complexes. *Structure.* 13:373–380.

40. Tama, F., and C. L. Brooks, III. 2006. Symmetry, form, and shape: guiding principles for robustness in macromolecular machines. *Annu. Rev. Biophys. Biomol. Struct.* 35:115–133.

41. Bahar, I., A. R. Atilgan, and B. Erman. 1997. Direct evaluation of thermal fluctuations in proteins using a single-parameter harmonic potential. *Fold. Des.* 2:173–181.

42. Atilgan, A. R., S. R. Durell, …, I. Bahar. 2001. Anisotropy of fluctuation dynamics of proteins with an elastic network model. *Biophys. J.* 80:505–515.

43. Micheletti, C., P. Carloni, and A. Maritan. 2004. Accurate and efficient description of protein vibrational dynamics: comparing molecular dynamics and Gaussian models. *Proteins.* 55:635–645.

44. Tama, F., F. X. Gadea, …, Y. H. Sanejouand. 2000. Building-block approach for determining low-frequency normal modes of macromolecules. *Proteins.* 41:1–7.

45. Doruker, P., R. L. Jernigan, and I. Bahar. 2002. Dynamics of large proteins through hierarchical levels of coarse-grained structures. *J. Comput. Chem.* 23:119–127.

46. Kurkcuoglu, O., P. Doruker, and R. L. Jernigan. 2004. Mixed levels of coarse-graining of large proteins using elastic network model succeeds in extracting the slowest motions. *Polymer (Guildf.).* 45:649–657.

47. Keskin, O., I. Bahar, …, R. L. Jernigan. 2002. Molecular mechanisms of chaperonin GroEL-GroES function. *Biochemistry.* 41:491–501.

48. Chennubhotla, C., and I. Bahar. 2007. Markov methods for hierarchical coarse-graining of large protein dynamics. *J. Comput. Biol.* 14:765–776.

49. Yang, Z., P. Májek, and I. Bahar. 2009. Allosteric transitions of supramolecular systems explored by network models: application to chaperonin GroEL. *PLOS Comput. Biol.* 5:e1000360.

50. Yildirim, Y., and P. Doruker. 2004. Collective motions of RNA polymerases. Analysis of core enzyme, elongation complex and holoenzyme. *J. Biomol. Struct. Dyn.* 22:267–280.

51. Tama, F., M. Valle, …, C. L. Brooks, 3rd. 2003. Dynamic reorganization of the functionally active ribosome explored by normal mode analysis and cryo-electron microscopy. *Proc. Natl. Acad. Sci. USA.* 100: 9319–9323.

52. Wang, Y., A. J. Rader, …, R. L. Jernigan. 2004. Global ribosome motions revealed with elastic network model. *J. Struct. Biol.* 147: 302–314.

53. Kurkcuoglu, O., P. Doruker, …, R. L. Jernigan. 2008. The ribosome structure controls and directs mRNA entry, translocation and exit dynamics. *Phys. Biol.* 5:046005.

54. Yang, Z., I. Bahar, and M. Widom. 2009. Vibrational dynamics of icosahedrally symmetric biomolecular assemblies compared with predictions based on continuum elasticity. *Biophys. J.* 96:4438–4448.

55. Berendsen, H. J. C., and S. Hayward. 2000. Collective protein dynamics in relation to function. *Curr. Opin. Struct. Biol.* 10:165–169.

56. Sanejouand, Y. H. 2006. Functional information from slow mode shapes. *In* Normal Mode Analysis. Theory and Applications to Biological and Chemical Systems. Q. Cui and I. Bahar, editors. Chapman & Hall/CRC, New York.

57. Lammens, A., A. Schele, and K. P. Hopfner. 2004. Structural biochemistry of ATP-driven dimerization and DNA-stimulated activation of SMC ATPases. *Curr. Biol.* 14:1778–1782.

58. Bates, P. A., L. A. Kelley, …, M. J. Sternberg. 2001. Enhancement of protein modeling by human intervention in applying the automatic programs 3D-JIGSAW and 3D-PSSM. *Proteins.* (*Suppl 5*):39–46.

59. Berman, H. M., J. Westbrook, …, P. E. Bourne. 2000. The protein data bank. *Nucleic Acids Res.* 28:235–242.

60. Whitby, F. G., and G. N. Phillips, Jr. 2000. Crystal structure of tropomyosin at 7 Ångstroms resolution. *Proteins.* 38:49–59.

61. Beasley, M., H. Xu, …, M. McKay. 2002. Conserved disruptions in the predicted coiled-coil domains of eukaryotic SMC complexes: implications for structure and function. *Genome Res.* 12:1201–1209.

62. Kurkcuoglu, O., O. T. Turgut, …, P. Doruker. 2009. Focused functional dynamics of supramolecules by use of a mixed-resolution elastic network model. *Biophys. J.* 97:1178–1187.

63. Case, D. A., T. A. Darden, …, P. A. Kollman. 2006. AMBER 9. University of California at San Francisco, San Francisco, CA.

64. Duan, Y., C. Wu, …, P. Kollman. 2003. A point-charge force field for molecular mechanics simulations of proteins based on condensed-phase quantum mechanical calculations. *J. Comput. Chem.* 24:1999–2012.

65. Akten, E. D., S. Cansu, and P. Doruker. 2009. A docking study using atomistic conformers generated via elastic network model for cyclosporin A/cyclophilin A complex. *J. Biomol. Struct. Dyn.* 27:13–26.

66. Phillips, J. C., R. Braun, …, K. Schulten. 2005. Scalable molecular dynamics with NAMD. *J. Comput. Chem.* 26:1781–1802.

67. MacKerell, Jr., A. D., T. D. Bashford, …, M. Karplus. 1998. All-atom empirical potential for molecular modeling and dynamics studies of proteins. *J. Phys. Chem. B.* 102:3586–3616.

68. Mackerell, Jr., A. D., M. Feig, and C. L. Brooks, 3rd. 2004. Extending the treatment of backbone energetics in protein force fields: limitations of gas-phase quantum mechanics in reproducing protein conformational distributions in molecular dynamics simulations. *J. Comput. Chem.* 25:1400–1415.

69. Amadei, A., M. A. Ceruso, and A. Di Nola. 1999. On the convergence of the conformational coordinates basis set obtained by the essential dynamics analysis of proteins' molecular dynamics simulations. *Proteins.* 36:419–424.

70. Tama, F., and Y. H. Sanejouand. 2001. Conformational change of proteins arising from normal mode calculations. *Protein Eng.* 14:1–6.

71. Muthurajan, U. M., Y. Bao, …, K. Luger. 2004. Crystal structures of histone Sin mutant nucleosomes reveal altered protein-DNA interactions. *EMBO J.* 23:260–271.

72. Aleksiev, T., R. Potestio, …, C. Micheletti. 2009. PiSQRD: a web server for decomposing proteins into quasi-rigid dynamical domains. *Bioinformatics.* 25:2743–2744.

73. Painter, J., and E. A. Merritt. 2006. Optimal description of a protein structure in terms of multiple groups undergoing TLS motion. *Acta Crystallogr. D Biol. Crystallogr.* 62:439–450.

74. Gilbert, S. P., M. R. Webb, …, K. A. Johnson. 1995. Pathway of processive ATP hydrolysis by kinesin. *Nature.* 373:671–676.

75. Nooren, I. M. A., and J. M. Thornton. 2003. Diversity of protein-protein interactions. *EMBO J.* 22:3486–3492.

76. Caffrey, D. R., S. Somaroo, …, E. S. Huang. 2004. Are protein-protein interfaces more conserved in sequence than the rest of the protein surface? *Protein Sci.* 13:190–202.